The Dark Side of Radio Jets In Powerful Extended Sources

ALAN H. BRIDLE
National Radio Astronomy Observatory

Abstract The properties of the known kiloparsec-scale counterjets in powerful sources are reviewed. Most of them are not "fainter replicas" of the brighter "main" jets. This makes it difficult to quantify jet "sidedness" uniquely, as required to test simple relativistic-jet models. In a complete sample of extended 3CR quasars, the best counterjet candidates are found opposite parts of the main jets that are "bent or broken". This suggests that counterjet emission is detected where the underlying beams interact strongly with their environment, and further complicates tests of relativistic-jet models using data from the "dark side". In a few sources, the observed jet-counterjet relationships match those expected of "born-again" relativistic jets. New observations that could clarify jet-counterjet relationships in powerful sources are suggested.

1. Introduction

The earliest "beam" models of energy transport in extragalactic sources (Blandford and Rees 1974; Scheuer 1974) assumed that the central engines in active galactic nuclei produce pairs of collimated outflows (beams) that are side-to-side symmetric and continuous. "Twin" beams were a natural postulate because many powerful radio sources have "non-identical twin" lobes, different in detailed structure but similar in total power. The first glimpses of elongated "jets" in radio galaxies were taken as evidence for the twin beams, even though some of these jets were seen on only one side of their parent galaxy's nucleus (e.g., M 87—Baade and Minkowski 1954; 3C 219—Turland 1975; 0844+319—van Breugel and Miley 1977) and others were clearly asymmetric (e.g., 3C 66B—Northover 1973).

On scales of a few kiloparsecs and above, "two-sidedness" (by my $< 4:1$ intensity-ratio criterion) is common only in the jets of sources with total lobe powers $P_{\rm lobe} < 10^{25}$ W Hz^{-1} at 1.4 GHz (for $H_0 = 100$ km s^{-1} Mpc^{-1}, $q_0 = 0.5$). At these powers, most sources have edge-darkened, plume-like structures (FR class I, Fanaroff and Riley 1974). Convincing *counterjets* have been hard (but not impossible) to find in the higher-power edge-brightened FR II doubles, even on radio images with high dynamic range. This poses an important question:

Parsec-Scale Radio Jets, ed. J. A. Zensus and T. J. Pearson

if FR II sources are powered by twin beams, why are their large-scale jets "bright" on one side (the "main jet") and "dark" on the other (the "counterjet")?

Most *parsec*-scale jets are "one-sided" in these terms, and jet brightness asymmetries on parsec and kiloparsec scales are strongly coupled. Where "one-sided" jets are known on both scales in the same source, the brighter (or only) kiloparsec-scale jet is always a plausible continuation of the brighter (or only) parsec-scale jet on the same side of the core. The coupling of the parsec and kiloparsec-scale asymmetries justifies reviewing what we know about the "dark sides" of *kiloparsec*-scale jets in strong sources at a workshop on parsec-scale phenomena. But before I describe what recent VLA observations have told us about counterjets in FR II sources, let me recall possible interpretations of the intensity asymmetry.

There are at least three views about what might be happening on the "dark side" of the kiloparsec-scale jets in FR II sources:

(*a*) *Nothing*, i.e., "what we see is what's happening". On this view, the asymmetry of the synchrotron emission from the jets is a manifestation of an asymmetry in the rate of energy transport by the beams. The central engine intrinsically supplies less power, or even no power, to the "dark side". The engine must therefore reverse its preference ("flip-flop") occasionally to form sources with two lobes. On this view, the postulate of steady, continuous twin beams would be doubly incorrect, both about steadiness and about twinning.

(*b*) *There is an active beam on the dark side but its synchrotron emissivity is low*, i.e., the energy pipeline is more efficient on the dark side than on the bright side. On this view, the two beams may transport the same power, but the beam on the dark side may (for example) interact less with surrounding gas, or may contain fewer relativistic electrons or a different magnetic field strength and configuration, than the other. On this view, the brightness asymmetries of jets in FR II sources may be induced by "minor" asymmetries in the beam environments or in their content of relativistic particles and fields.

(*c*) *There is a beam on the dark side* that is intrinsically identical to the beam on the bright side, *but its synchrotron emission is directed away from us by bulk relativistic motion.* On this view, the "one-sidedness" of the jets in FR II sources implies that the beam velocities remain at least mildly relativistic to kiloparsec scales. This is a simple extrapolation to larger scales of the popular models for one-sidedness and superluminal motion in parsec-scale jets.

These three views represent three different simplifications; there are others that I will not discuss here. Until recently, our view of jet-counterjet relationships in powerful sources was unfettered by detections

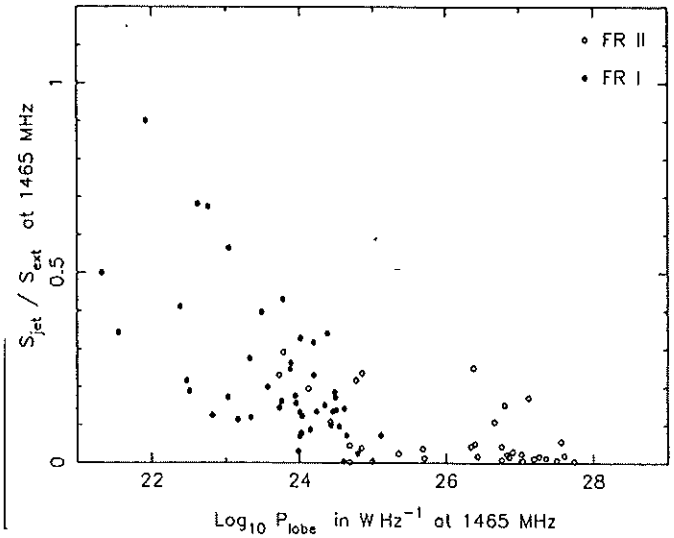

Figure 1 A plot of jet prominence versus total lobe power for 104 "classical" FR I and FR II sources. Jet prominence is measured here by the ratio of integrated flux density in the brighter jet to the total extended flux density (all emission outside the unresolved core). This quantity cannot exceed unity. All flux densities have been estimated at 1465 MHz.

of the counterjets. I will review how deep VLA imaging of powerful sources is beginning to change this for sources with lobe powers $P_{\rm lobe} > 10^{26}$ W Hz^{-1} at 1.4 GHz (well above the usual power regime of two-sided jets and edge-darkened lobes).

2. Relative Prominence of Jets and Counterjets

The "two-sided" jets in weak sources often provide several tens of per cent of the total extended emission, but in "classical doubles" with $P_{\rm lobe} > 10^{25}$ W Hz^{-1} at 1.4 GHz, the main jets rarely provide more than about 15% of the total, and often much less (Figure 1). In Figure 1's sample of 104 FR I and FR II sources, the most prominent jet at $P_{\rm lobe} > 10^{26}$ W Hz^{-1} is in 4C 32.69; its unusual prominence may account for this jet's early discovery (Potash and Wardle 1980).

There are prominent kiloparsec-scale jets in some powerful sources, however. Figure 2 plots the ratio of jet to total extended emission for 19 sources whose extended structures are *not* obvious "classical" FR I or FR II types. The seven sources coded "O" have only one detected *lobe*, often diffuse and devoid of hotspots. The twelve sources coded "C" have complex extended emission in all directions around the core (Peter Wilkinson aptly described such structures here as "fried eggs thrown at a wall") and are smaller on average than the FR II sources. The "C"

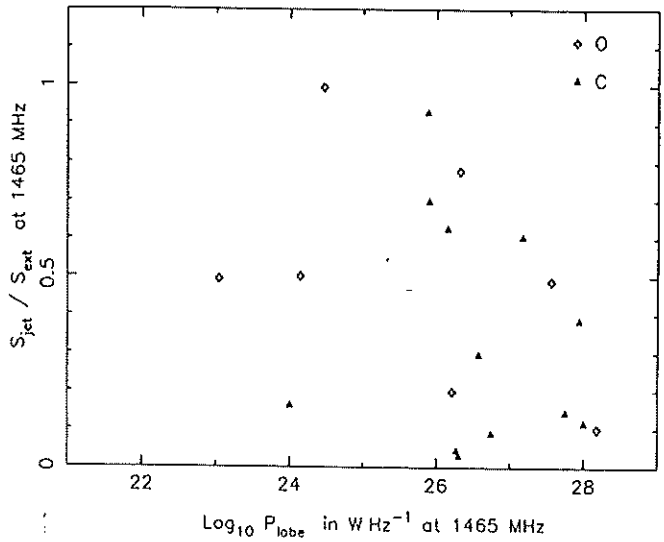

Figure 2 As in Figure 1, but for 19 sources whose structures (after subtracting their jets) are not obviously "classical" FRI or FRII types. Type O (*crosses*) have only one detected lobe to one side of the core; type C (*triangles*) have complex extended emission in all directions around the core. Note the preponderance of prominent jets at high lobe powers relative to Figure 1.

sources could be FRI or FRII objects seen almost end-on. They may also be intrinsically small, complex sources, however.

Figure 3 plots the ratio of integrated counterjet emission to total extended emission for 48 counterjets whose integrated flux densities can be derived from the literature or my own data. Most counterjets in sources with $P_{\rm lobe} > 10^{26}$ W Hz^{-1} at 1.4 GHz contain only a few per cent or less of the total extended emission. This is why they have been so elusive until recently: their small fractional powers make them *extremely* hard to detect at the resolutions needed to demonstrate that they are indeed counterjets. Notice also that *whatever makes the main kiloparsec-scale jets so prominent in sources with "nonclassical" type C structures does not enhance their counterjets equally.* (The type O sources have no counterjet by definition.)

The trends shown in Figures 1, 2, and 3—decreasing jet prominence with increasing lobe power in FRI and FRII sources, increased prominence of jets but not counterjets in the C sources—are all expected if beam velocities are mildly relativistic on kiloparsec scales at high lobe powers but not at low, and if the FRII sources are (on average) nearer the plane of the sky than O and C sources with similar lobe powers. The O and C sources also show a positive correlation between core prominence and jet prominence and a negative correlation between

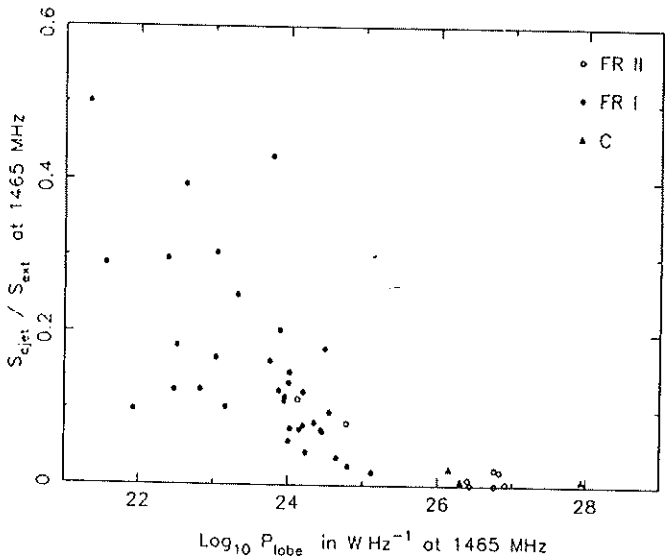

Figure 3 A plot of counterjet prominence versus total lobe power for 48 FRI, FRII, and C sources for which integrated counterjet flux densities are available. As in Figure 1, "prominence" is measured by the ratio of integrated (counter)jet flux density to the total extended flux density at 1465 MHz. This quantity cannot exceed 0.5. The vertical scale is twice that of Figures 1 and 2.

jet prominence and projected linear size (Bridle 1988). These trends encourage, but do not mandate, the relativistic-jet view of the "dark side". If final beam velocities are indeed higher at higher beam powers and lobe powers, jet prominence and jet sidedness on kiloparsec scales may correlate positively with maximum pattern speeds on parsec scales. It will be interesting to look for such correlations when both types of data are available for source samples that represent a wide range of lobe powers.

3. Counterjets in Powerful Radio Galaxies

Seven cases are known and four have been quantified. In order of increasing lobe power, the four are:

3C 288 (Bridle *et al.* 1989): $P_{lobe} = 10^{26.36}$ W Hz^{-1}, $P_{jet} = 10^{24.36}$ W Hz^{-1}, $P_{cjet} = 10^{23.68}$ W Hz^{-1} at 1.4 GHz. The lobes barely qualify as an FRII structure and the hotspots are ill-defined, but this could be an FRII source near the line of sight. The jet can be traced for only 6 kpc, about one-third of the way into its lobe. The counterjet is an elongated knot whose peak (2.8 kpc from the core) is near its outer tip. (This feature does not meet my $> 4:1$ elongation criterion for "jethood" but its location on the jet axis and elongation along it both support identifying it as the brightest part of the counterjet.) The mean spectral index of the counterjet between 0.4 and 15 GHz is -1.23, while that of the main jet is -0.88. The intensity ratio between the jet and counterjet is therefore frequency-dependent; this jet system is "two-sided" below 3 or 4 GHz and "one-sided" at higher frequencies.

3C 219 (Bridle, Perley, and Henriksen 1986): $P_{\rm lobe} = 10^{26.43}$ W Hz^{-1}, $P_{\rm jet} = 10^{24.68}$ W Hz^{-1}, $P_{\rm cjet} = 10^{23.22}$ W Hz^{-1} at 1.4 GHz. The main jet "disappears" 36 kpc from the core, less than one-third of the way towards the hotspot on its side of the source. The counterjet is a knot that is elongated along the jet axis and whose peak (9.6 kpc from the core) is near its outer tip. As in 3C 288, it does not separately meet my elongation criterion for "jethood" but its location and axis of elongation make it likely that it is the brightest part of the counterjet. The lobe hotspots are well-defined, but are both large and relaxed. 3C 288 and 3C 219 may both contain examples of "born-again" relativistic jets (see below).

3C 438 (R. Laing, personal communication): At 1.4 GHz, $P_{\rm lobe} = 10^{26.82}$ W Hz^{-1}, $P_{\rm jet} = 10^{25.19}$ W Hz^{-1}, $P_{\rm cjet} = 10^{25.11}$ W Hz^{-1}. The lobes are edge-brightened but the source lacks compact hotspots. The similarity of the jet and counterjet, both about 24 kpc long, make this source a strong exception to the general trend of jet symmetries. Both jets meet all my elongation and brightness contrast criteria for "jethood".

Cygnus A (Carilli 1989): At 1.4 GHz, $P_{\rm lobe} = 10^{27.74}$ W Hz^{-1}, $P_{\rm jet} = 10^{24.57}$ W Hz^{-1}, $P_{\rm cjet} = 10^{24}$ W Hz^{-1}. The counterjet, as imaged by Carilli, meets all of my criteria for "jethood". Carilli traces it for about 8 kpc near the core and along the outer 26 kpc of a curved path toward the most compact hotspot in the east lobe. Both the jet and the counterjet brighten and bend as they enter the brighter parts of their lobes; the main jet also bifurcates (limb brightens) here, suggesting a strong interaction with the lobe (cocoon) material.

There are three other powerful radio galaxies with detectable counterjet emission: 3C 218 (G. Taylor and R. Perley, private communication), 3C 341 (Bridle and Perley 1984) and 3C 348 (Dreher and Feigelson 1984). 3C 218 has an FR I structure despite its high total power. In 3C 341, the jet and counterjet are hard to distinguish from highly elongated lobes. In 3C 348, a counterjet that is straight between 16 and 36 kpc from the core breaks up into rings further into the lobe. No reliable jet or counterjet flux densities are available for these sources, which have $P_{\rm lobe} = 10^{26.30}$ W Hz^{-1}, $10^{26.75}$ W Hz^{-1}, and $10^{27.1}$ W Hz^{-1} respectively at 1.4 GHz.

4. Counterjets in Extended 3CR Quasars

Bridle *et al.* (1990) have made sensitive (20 μJy per beam) 4.9 GHz images of 12 of the 19 3CR quasars with flux densities > 0.3 Jy at 4.9 MHz and largest angular sizes $> 10''$, using long integrations combining the VLA A and B configurations (FWHMs near $0\farcs36$). The 12 sources (Table 1) were selected because they fitted a common VLA observing schedule, not by their jet or core properties. Jets were detected in all twelve. None of the twelve has a counterjet that clearly meets my criteria for "jethood" ($> 4:1$ elongation and brightness contrast relative to other lobe emission) but six (identified by "C = Y" in Table 1) have pieces of putative counterjet emission. Table 1 summarizes these results in order of increasing lobe power at 4.9 GHz, giving the most "generous" assessment of which pieces may be jet and counterjet in each case. Some notes on the properties of the individual jets and counterjets revealed by this survey follow; these are given in detail to illustrate the many problems of quantifying jet/counterjet relationships.

3C 215: Both lobes look disturbed; one has an FR I-like plume. The knotty jet has two sharp bends before it ends 40 kpc from the core in a curved hotspot. A

Table 1 Jet and Counterjet Quantities in Extended 3CR Quasars

Source	(1) C	(2) P_l	(3) P_c	(4) P_j	(5) P_{cj}	(6) *LLS*	(7) Q_i	(8) Q_n	(9) f_c	(10) f_j	(11) f_{cj}
3C 215	Y	25.90	24.55	24.95	23.95	196	9.9	16.8	0.045	0.113	0.0114
3C 249.1	Y	25.90	24.93	24.81	24.01	149	6.3	6.6	0.108	0.082	0.013
3C 334	Y	26.28	25.75	25.04	24.00	215	10.8	15.6	0.298	0.058	0.0053
3C 351	Y	26.31	24.07	24.29	22.49	229	63	18	0.0057	0.0094	0.0002
3C 263	N	26.71	25.96	24.77	<23.28	200	>31	>40	0.180	0.0115	<0.0004
3C 175	N	26.72	25.29	25.22	<23.00	212	>164	>136	0.037	0.032	<0.0002
3C 204	N	26.75	25.70	25.25	<23.51	159	>55	>62	0.089	0.032	<0.0006
3C 9	Y	26.90	25.54	27.41	25.63	57	60	34	0.043	3.20	0.054
3C 208	N	26.96	25.98	25.58	<24.28?	60	>20?	>18?	0.105	0.042	<0.0021?
3C 336	N	26.99	25.42	25.07	<24.25	118	>6.5	>16	0.027	0.0119	<0.0018
3C 68.1	Y	27.27	24.40	24.93	24.87	228	1.2	0.6	0.0013	0.0045	0.0039
3C 432	N	27.30	25.62	24.61	<23.83	63	>6.0	>4.8	0.021	0.0020	<0.0003

Explanation: (1) C: Counterjet detected (Yes or No). (2) P_l: $\log_{10}$(lobe power in W Hz^{-1} at 4.9 GHz); lobe power is total source power minus jet, counterjet, and core contributions. (3) P_c: $\log_{10}$(core power in W Hz^{-1} at 4.9 GHz); the core defined as central unresolved component as seen by VLA A-configuration at 4.9 GHz. (4) P_j: $\log_{10}$(jet power in W Hz^{-1} at 4.9 GHz); the jet includes all emission on jet path between core and presumed terminal hotspot, corrected for background from lobe based on equal-area adjacent patches. (5) P_{cj}: $\log_{10}$(counterjet power in W Hz^{-1} at 4.9 GHz); the counterjet includes all emission that could plausibly be associated with a counterjet along path between core and presumed terminal hotspot, if any. (6) *LLS*: largest linear size (diameter) of source, in kpc. (7) Q_i: ratio of integrated flux densities (jet/counterjet). (8) Q_n: ratio of flux densities per unit length (jet/counterjet). (9) f_c: core prominence—ratio of flux densities core/lobes at 4.9 GHz; both lobes, excluding jet and counterjet. (10) f_j: jet prominence—ratio of integrated flux densities jet/lobes at 4.9 GHz. (11) f_{cj}: counterjet prominence—ratio of integrated flux densities counterjet/lobes at 4.9 GHz.

slender counterjet can be traced for about 70 kpc to a "warm spot" in its lobe after an initially "blank" 10 kpc. The first detectable counterjet knot is approximately opposite the first jet knot, and both precede sharp bends with "S" symmetry across the core. The main uncertainty in the integrated emission from the counterjet is the correction for confusion by the lobe, because the brightness contrast between them is poor.

3C 249.1: The jet ends 22 kpc from the core at a hotspot near an inner edge of its lobe, and has several changes in direction. There is weak narrow counterjet emission opposite the initial 11 kpc of the jet, where the jet brightness decreases rapidly. There are two extended arcs of emission in the counterjet lobe in the next 11 kpc opposite the outer part of the main jet. These arcs are similar in size and luminosity to the "rings" in Hercules A (Dreher and Feigelson 1984). The major uncertainty in the counterjet intensity is whether to count these arcs as extended parts of the counterjet. The initial 11 kpc segment of the counterjet meets my elongation criterion for "jethood" but has marginal brightness contrast relative to other features of its lobe.

3C 351: The jet is a train of knots within 7 kpc of the core, whose brightnesses rapidly decrease with increasing distance. A marginally detected curved ray that may be additional jet emission extends for 60 kpc through its lobe toward a prominent compact hotspot. The counterjet candidate is a weak knot 2.2 kpc from the core that does not separately meet my elongation criterion for "jethood".

3C 334: The main jet is straight for about 60 kpc, then bends sharply round the edge of the east lobe. Near the bend it meets a highly polarized "ray" that

touches the lobe boundary. There is no detectable counterjet emission on the path opposite the straight 60 kpc of the main jet. Just beyond 60 kpc along this path, opposite the sharp bend in the main jet, is an elongated knot. This knot is linked by a 30-kpc curved "ray" to the most compact "hotspot" in the west lobe. It is not clear whether this second "ray" is a 30-kpc segment of the counterjet or a lobe boundary feature (like the ray in the jetted lobe). Table 1 assumes that both the ray and the first knot are counterjet emission.

3C 263: A straight jet 63 kpc long points toward a compact hotspot complex that is elongated toward it. There is no detectable counterjet.

3C 175: A continuous jet, initially straight but gradually curving, runs for 100 kpc from the core to a recessed hotspot in the lobe. The first 34 kpc of the counterjet path is uncontaminated by lobe emission and contains no counterjet candidate. Within this first 34 kpc of the core, the lower limit to the jet/counterjet intensity ratio is $> 33 : 1$, significantly less than the limit for the whole path (Table 1). The hotspot in the counterjet lobe is compact and protrudes through the lobe wall. This strongly suggests ongoing, or recent, energy transport on the "dark side" of this source.

3C 204: The jet contains five bright knots in fainter underlying emission extending on a straight path for 45 kpc from the core toward a recessed hot spot. The first 36 kpc of the putative counterjet path are unconfused and contain no significant emission; the jet/counterjet intensity ratio in this 36 kpc is $> 43 : 1$, less than the limit given for the whole path in Table 1.

3C 9: There are 22 kpc of bent jet before a knot that could either be the brightest feature of the jet or a recessed hotspot. A collimated stream continues beyond it. If the entire stream is "jet", the jet has 365 mJy and the lobe only 11 mJy; but a case can be made for assigning only 75 mJy to the jet and 301 mJy to the lobe. On the counterjet side is a knot 4 kpc from the core and a 15-kpc filament that may be a continuation of the counterjet into the lobe. The "minimum" counterjet emission is 0.22 mJy, but the "maximum" is 6.1 mJy. The jet/counterjet intensity ratio is uncertain by a factor of over 100; Table 1 assumes maximal contributions from both the jet and the counterjet. The ratio of intensities between the initial counterjet knot and the opposite segment of the jet is only 5:1, much less than the integrated ratio in Table 1.

3C 208: The jet has several bright knots in extended underlying emission extending 20 kpc from the core to a recessed hotspot in the west lobe. The east lobe has an almost-detached resolved extension that could either be a poorly collimated counterjet or (more likely) part of the lobe "cocoon". There is no unambiguous narrow counterjet emission, but the east lobe extension confuses estimates of the upper limit (hence the "?" entries in Table 1).

3C 336: The jet is straight for about 21 kpc, then deflects into the south lobe at an oblique knot. There is no obvious counterjet, though a knot and "hook" on the north side of the north lobe could be examples of a "wall jet" (e.g., Wilson 1989).

3C 68.1: This source tests any jet classification language! Pieces of both jets are detected, and their integrated flux densities are similar (3.6 and 3.1 mJy for the north and south jets respectively). The north jet is faint and extended but the south jet is bright and compact (it is elongated along the major axis of the source but does not meet my $> 4 : 1$ criterion for "jethood"). The south jet would be the counterjet using integrated flux density as the discriminant, the north jet would be the counterjet using surface brightness as the discriminant. This is the only candidate "two-sided" jet system in this 3CR quasar sample. It is also the source with the lowest core prominence and the second-lowest jet prominence in the sample.

3C 432: We detect the brightest segment of a jet about 9 kpc from the core, one-third of the way to the outer edge of the lobe. There is no detectable counterjet.

Aside from 3C 68.1, neither of the jet/counterjet intensity ratios Q given in Table 1 correlates with core prominence or with jet prominence (relative to the lobes), or anticorrelates with projected linear size, as

expected on the simplest relativistic-jet models of "one-sidedness". As none of the counterjet candidates is a faint replica of its main jet, the intensity ratios may be determined by factors that are not included in the simple models, however. There is also no evidence in this small sample for intrinsic differences between the jetted and unjetted lobes: the main jets do not systematically point toward the brighter lobe, or toward the shorter arm of the source. In all but 3C 175, the main jet points toward the hotspot with the highest surface brightness, but this result may depend on resolution.

5. Counterjets in Superluminal Sources

There are two large-scale counterjet candidates in quasars that have $P_{\rm lobe} > 10^{26}$ W Hz^{-1} at 1.4 GHz and which exhibit superluminal motions on parsec scales:

3C 345 (Kollgaard, Wardle, and Roberts 1989): $P_{\rm lobe} = 10^{26.13}$ W Hz^{-1}, $P_{\rm jet} = 10^{26.37}$ W Hz^{-1}, $P_{\rm cjet} = 10^{24.9}$ W Hz^{-1}, scaled to 1.4 GHz. The counterjet candidate extends from the core in a direction nearly opposite to that of the most recent expulsion of a parsec-scale feature, roughly at right angles to the axis of the brightest part of the main jet. It may however be an artifact of under-sampling the known larger-scale structure on this side of the source (Wardle, personal communication).

4C 73.18 = 1928+738 (Johnston *et al.* 1987): $P_{\rm lobe} = 10^{26.30}$ W Hz^{-1}, $P_{\rm jet} = 10^{24.8}$ W Hz-1, $P_{\rm cjet} = 1024.0$ W Hz^{-1}, scaled to 1.4 GHz. Both the jet and the counterjet brighten where bends begin. The peak of the counterjet opposes a gap in the straight initial segment of the main jet, unlike the sources in our 3CR quasar survey. The structure is not well resolved, however, so the jet trajectory may yet prove to be more complex.

6. Commentary

(*a*) Most (but not all) of the counterjet candidates in FR II sources are found opposite parts of the main jets that are "bent or broken", i.e., strongly curved, or rapidly changing in brightness, or both. Counterjet emission is especially hard to find opposite the long, straight segments of the 3CR quasar jets. The counterjet emission may therefore be showing up most readily in parts of sources where the beams interact strongly with their environment. (There may be subtle evidence for this in Cygnus A, where the apparent bifurcation of the outer jet could be a signal of strong interactions in a boundary layer.)

If counterjets are brightest where they are strongly interacting, it is unlikely that flow velocities are constant in either magnitude or direction where most jet/counterjet intensity ratios can now be directly measured. If the kiloparsec-scale flow velocities are often relativistic in FR II sources, counterjets may be detectable only where unfavorable beaming factors are removed on the receding side by perturbing the flows. This

must complicate, and may prevent, the use of global jet/counterjet intensity ratios for tests of "unified schemes" that assume unique values of the Lorentz factor in each beam.

(*b*) The apparent "disappearance" of the jets in 3C 219, 3C 288, and 3C 351 on the way into their lobes might be due to variations in efficiency along steady underlying beams (paralleling the view *b* of the "dark side", Section 1). It may however be significant that the counterjets appear shorter than the main jets in all three sources. Both this geometrical asymmetry and the end-brightening of the counterjets in 3C 219 and 3C 288 are expected in "born-again" relativistic jets (Bridle, Perley, and Henriksen 1986; Bridle 1988; Bridle *et al.* 1989), i.e., in relativistic jets whose central engines show long-term variability and have recently "restarted". In the "born- again" jet model, the tips of both jets are the sites of outward-moving shocks that are symmetric in the frame of the active nucleus; we see the counterjet at an earlier age, and thus apparently foreshortened, because of travel time effects. (This model should be distinguished from the non-relativistic "flip-flop", which does not predict unique relationships between the lengths of the counterjet and the main jet). In the "born-again" jet model, the outer tip of the counterjet is its brightest part because an unfavorable Doppler factor is reduced or removed there. As shown in Jack Burns's poster at this Workshop (Burns and Clarke, page 260), the hotspots in sources with "born-again" jets should relax soon after the momentum and energy supply from the central engine is temporarily withdrawn. All the hotspots in 3C 288 and 3C 219 are indeed relaxed, but this is not unusual for sources with these lobe powers. In 3C 351, the jetted hotspot is compact, and a faint jet segment still feeds it, so this hotspot may not have been fully cut off.

If "born-again" counterjets are made visible by perturbations at their terminal shocks, a diagnostic for this model may be the presence of emission from the associated stand-off shock. The stand-off shock travels in a cocoon that contains relativistic electrons and fields left behind by earlier activity, so it may be detectable in some cases. (In discussion at this meeting, Patrick Leahy showed a possible example of such "standoff shock" emission around the abbreviated main jet in 3C 33.1; see also Rudnick 1984).

(*c*) Attempts to estimate integrated counterjet powers are complicated by problems both of counterjet recognition (e.g., confusion by lobe filaments and "rays" as in 3C 334, questions of whether extended features on one side should be equated to compact knots on the other as in 3C 249.1) and of correcting faint features for a spatially variable lobe background. My colleagues and I are still assessing these errors for our 3CR quasar sample (so Table 1 is preliminary!).

(*e*) Jet/counterjet ratio measurement is even harder, because the counterjets are not faint replicas of the main jets. The ratio of peak intensities is easily found but is probably not useful: knot-to-knot brightness differences may tell us more about local disturbances in the flows than about global parameters. The integrated flux density ratios are hard to assess if no counterjet is detected—if the main jet is curved, or abbreviated, over what size and shape of region should the dark side be integrated? For "born-again" relativistic jets, brightness asymmetries would be over-estimated by integrating the apparently foreshortened counterjet over the same length as the main jet, or over the whole path to the hotspot. We face a dilemma: can we pose questions about jet/counterjet intensity ratios properly without having an underlying model (i.e., the "answers" to these questions) already?

(*f*) If all the putative counterjets in Table 1 are correctly identified and measured, the statistics of jet sidedness in our 3CR quasar sample are compatible (at about the one-sigma level) with the statistics expected for Doppler favoritism in an isotropically oriented group of sources with unidirectional beam velocity fields, whatever the Lorentz factors of the beams. The joint statistics of sidedness and apparent linear size may however be incompatible with random orientation and simple Doppler favoritism at the two-sigma level—there are awkwardly many large sources in the sample with high jet/counterjet ratios (3C 175, 3C 204, 3C 263, and 3C 351). The statistical significance of this depends on how we treat the systematic uncertainties in the ratios, and my co-conspirators and I are still evaluating this. Note that if the counterjet assessments in Table 1 are too generous, the jet/counterjet intensity ratios are higher than given there, so the conflict with random selection from a Doppler-boosted isotropic sample will be more significant.

(*g*) The absolute powers of the counterjet candidates in the FR II sources exceed the jet and lobe powers of most FR I sources. If these candidates are indeed the brightest parts of counterjets (i.e., they are not merely confusing lobe features), the jet-counterjet pairs in these sources cannot be Doppler-enhanced beams with low intrinsic radio powers (similar to those in FR I sources).

(*h*) It will be hard for VLA data to refine the intensity ratio measurements given in Table 1, even with long observations. High sensitivity and dynamic range will be frustrated by confusion with lobe fine structure like filaments, and by problems of counterjet recognition similar to those described here.

(*i*) The possibility that counterjets have steeper spectra than the jets, as observed in 3C 288, may make jet/counterjet ratios (and "unified model" tests based on them) frequency-dependent. To explore this, more jets and counterjets in FR II radio galaxies and quasars should be

imaged at $< 1''$ resolution below 1 GHz. This is a task for MERLIN or for a composite VLA-VLBA array.

7. Conclusion

The glimpses of jet/counterjet relations offered by present VLA data do not discriminate clearly between the three views of the "dark side" that I summarized at the start of this paper. Views *a* and *b* are hard to test because they make few explicit predictions, but *a* (the flip-flop) is not encouraged by the presence of compact hotspots in unjetted lobes such as in 3C 175. The strength of view *c* (bulk relativistic effects) is that it offers a single coherent explanation of the global trends in jet sidedness, jet prominence and superluminal motions. A useful test for this view of the "dark side" may come from measuring jet and counterjet prominence in complete samples of powerful radio galaxies whose lobe powers are like those of the quasars in Table 1. If FR II quasars are more likely to be near the line of sight than FR II radio galaxies (Bridle and Perley 1984; Barthel 1989), the jets in such radio galaxies should be less prominent, and the jet/counterjet ratios smaller, than those in Table 1. As the VLA data suggest that interactions and perturbations of the flows may play an important role in determining their visibility, we may need to understand these interactions better before we can test relativistic-jet models convincingly with data from the "dark side". This conclusion may of course apply equally to the parsec-scale phenomena!

I thank Ron Ekers and Steve Gull for several provocative discussions of "born-again" relativistic jets. I am also grateful to John Wardle, David Hough, Peter Scheuer, Colin Lonsdale, David Clarke, and Tony Readhead for sharing their ideas about possible jet-counterjet relationships and about how to measure and test them. I hasten to add that this does not mean that they will agree with most, or even any, of what I have said here!

References

Baade, W., and Minkowski, R. 1954, *Astrophys. J.*, 119, 215.
Barthel, P. D. 1989, *Astrophys. J.*, 336, 606.
Blandford, R. D., and Rees, M. J. 1974, *Monthly Notices Roy. Astron. Soc.*, 169, 395.
Bridle, A. H. 1988, in *Active Galactic Nuclei*, ed. H. R. Miller and P. J. Wiita (Berlin: Springer), p. 329.
Bridle, A. H., Fomalont, E. B., Byrd, G. G., and Valtonen, M. J. 1989, *Astron. J.*, 97, 674.
Bridle, A. H., Hough, D. H., Burns, J. O., Laing, R. A., and Lonsdale, C. J. 1990, in preparation.
Bridle, A. H., and Perley, R. A. 1984, *Ann. Rev. Astron. Astrophys.*, 22, 319.
Bridle, A. H., Perley, R. A., and Henriksen, R. N. 1986, *Astron. J.*, 92, 534.
Carilli, C. L. 1989, Ph. D. thesis, Massachusetts Institute of Technology.
Dreher, J. W., and Feigelson, E. D. 1984, *Nature*, 308, 43.
Fanaroff, B. L., and Riley, J. M. 1974, *Monthly Notices Roy. Astron. Soc.*, 167, 31P.

Johnston, K. J., Simon, R. S., Eckart, A., Biermann, P., Schalinski, C., Witzel, A., and Strom, R. G. 1987, *Astrophys. J. (Letters)*, 313, L85.
Kollgaard, R. I., Wardle, J. F. C., and Roberts, D. H. 1989, *Astron. J.*, 97, 1550.
Northover, K. J. E. 1973, *Monthly Notices Roy. Astron. Soc.*, 165, 369.
Potash, R. I., and Wardle, J. F. C. 1980, *Astrophys. J.*, 239, 42.
Rudnick, L. 1984, in *Physics of Energy Transport in Extragalactic Radio Sources*, NRAO Workshop No. 9, ed. A. H. Bridle and J. A. Eilek (Green Bank: National Radio Astronomy Observatory), p. 35.
Scheuer, P. A. G. 1974, *Monthly Notices Roy. Astron. Soc.*, 166, 513.
Turland, B. D. 1975, *Monthly Notices Roy. Astron. Soc.*, 172, 181.
van Breugel, W. J. M., and Miley, G. K. 1977, *Nature*, 265, 315.
Wilson, M. J. 1989, in *Hot Spots in Extragalactic Radio Sources*, ed. K. Meisenheimer and H.-J. Röser (Berlin: Springer), p. 215.